



This is a post-refereeing final draft. When citing, please refer to the published version:

Di Prima, S., Stewart, R.D., Castellini, M., Bagarello, V., Abou Najm, M.R., Pirastru, M., Giadrossich, F., Iovino, M., Angulo-Jaramillo, R., Lassabatere, L., 2020. Estimating the macroscopic capillary length from Beerkan infiltration experiments and its impact on saturated soil hydraulic conductivity predictions. *Journal of Hydrology* 125159. <https://doi.org/10.1016/j.jhydrol.2020.125159>



## Estimating the macroscopic capillary length from Beerkan infiltration experiments and its impact on saturated soil hydraulic conductivity predictions

Simone Di Prima<sup>a,b\*</sup>, Ryan D. Stewart<sup>c</sup>, Mirko Castellini<sup>d</sup>, Vincenzo Bagarello<sup>e</sup>, Majdi R. Abou Najm<sup>f</sup>, Mario Pirastru<sup>a</sup>, Filippo Giadrossich<sup>a</sup>, Massimo Iovino<sup>e</sup>, Rafael Angulo-Jaramillo<sup>b</sup> and Laurent Lassabatere<sup>b</sup>

<sup>a</sup> Department of Agricultural Sciences, University of Sassari, Viale Italia, 39, 07100 Sassari, Italy.

<sup>b</sup> Univ Lyon, Université Claude Bernard Lyon 1, CNRS, ENTPE, UMR 5023 LEHNA, F-69518, Vaulx-en-Velin, France.

<sup>c</sup> School of Plant and Environmental Sciences, Virginia Polytechnic Institute and State University, Blacksburg, VA, United State.

<sup>d</sup> Council for Agricultural Research and Economics-Agriculture and Environment Research Center (CREA-AA), Via Celso Ulpiani 5, 70125 Bari, Italy.

<sup>e</sup> Department of Agricultural, Food and Forest Sciences, University of Palermo, Palermo, Italy.

<sup>f</sup> Department of Land, Air and Water Resources, University of California, Davis, CA 95616, United States.

\* Corresponding Author. E-mail: [sdiprima@uniss.it](mailto:sdiprima@uniss.it)

### Abstract

The macroscopic capillary length,  $\lambda_c$ , is a fundamental soil parameter expressing the relative importance of the capillary over gravity forces during water movement in unsaturated soil. In this investigation, we propose a simple field method for estimating  $\lambda_c$  using only a single-ring infiltration experiment of the Beerkan type and measurements of initial and saturated soil water contents. We assumed that the intercept of the linear regression fitted to the steady-state portion of the experimental infiltration curve could be used as a reliable predictor of  $\lambda_c$ . This hypothesis was validated by assessing the proposed calculation approach using both analytical and field data. The analytical validation demonstrated that the proposed method was able to provide reliable  $\lambda_c$  estimates over a wide range of soil textural characteristics and initial soil water contents. The field testing was performed on a large database including 433 Beerkan infiltration experiments, with the 99% of the experiments yielding realistic  $\lambda_c$  values. The generated  $\lambda_c$  values were then used in conjunction with four different methods for estimating saturated soil hydraulic conductivity,  $K_s$ . Estimated  $K_s$  values were close to those generated by a reference method, with relative error < 25% in nearly all cases. By comparison, assuming constant or soil-dependent  $\lambda_c$  values caused relative errors in  $K_s$  of up to 600%. Altogether, the proposed method constitutes an easy solution for estimating  $\lambda_c$ , which can improve our ability to estimate  $K_s$  in the field.

**Keywords:** infiltration, macroscopic capillary length, Beerkan, ring infiltrometer, hydraulic conductivity.

### 1. Introduction

The macroscopic capillary length,  $\lambda_c$  (L), was first described by Bouwer (1964) and expresses the relative importance of capillary over gravity forces during water movement in unsaturated soil (Raats, 1976). More specifically, low  $\lambda_c$  values (e.g.,  $0 < \lambda_c \leq 10$  mm) indicate a dominance of gravity over capillarity, and are typically found in coarse-textured or highly structured porous media (Reynolds et al., 2002). Alternately, high  $\lambda_c$  values (i.e.,  $> 1000$  mm) indicate dominance of capillarity over gravity, as found in many fine-textured or poorly structured porous media (Table 1).  $\lambda_c$  can also be used to estimate the macroscopic pore radius (i.e., the average radius of the pores that are active in flow) via the Young-Laplace equation (Kutilek and Nielsen, 1994), as suggested by Roulier et al. (2002). Because it indicates soil capillarity,  $\lambda_c$  is included in many infiltrometer methods for calculating  $K_s$  (e.g., Bagarello et al., 2004, 2014b, 2017; Elrick and Reynolds, 1992; Nimmo et al., 2009; Reynolds and Elrick, 1990; Stewart and Abou Najm, 2018a; Wu et al., 1999). It is thus important to accurately constrain  $\lambda_c$  under field conditions.

Previously developed methods to estimate  $\lambda_c$  have all presented some limitations. For instance, the two-ponding depths method by Reynolds and Elrick (1990) requires measuring steady state flow rates under two distinct water

ponding conditions, thus inducing considerable effort and experimental complexity. Bagarello et al. (2013) proposed empirical equations to estimate  $\lambda_c$ ; however, those results were site specific and therefore lacked generality. In addition, those authors used the cumulative linearization method (Smiles and Knight, 1976), which can fail in the presence of layered media, entrapped air, and vertical soil water content gradients (Vandervaere et al., 2000). Other methods are based on the analysis of transient state data, as for the case of the Method 1 by Wu et al. (1999) and Approach 2 by Stewart and Abou Najm (2018a). However, these approaches require accurate characterization of the transient state, which can be challenging under specific field conditions such as highly permeable, slightly sorptive and water-repellent soils (Di Prima et al., 2019). Therefore, alternative methods for estimating  $\lambda_c$  from simple and replicable infiltration experiments have the potential to substantially reduce the amount of work necessary to accurately estimate soil hydraulic properties.

The first objective of this investigation was to validate a simple field method to estimate  $\lambda_c$  that requires only a single-ring infiltration experiment taken to steady-state conditions (Lassabatere et al., 2006) and estimates for initial and saturated soil water contents. To meet this objective, we first developed the theoretical analysis for the estimation of  $\lambda_c$  from a single

**Table 1.** Soil capillarity categories suggested by Elrick and Reynolds (1992), and representative  $\lambda_c$  (mm) values. The suggested range values are also reported.

Soil capillarity category	Representative $\lambda_c$ (mm)	$\lambda_c$ range values
Very strong	$\geq 1000$	
Strong	250	$125 < \lambda_c < 1000$
Moderate	83	$42 < \lambda_c \leq 125$
Weak	28	$10 < \lambda_c < 42$
Negligible	$\leq 10$	

Beerkan run. We then validated the proposed method using analytically generated data, involving soils with different texture and initial water contents, and an empirical infiltration database that included data from 433 field measurements collected during previous investigations. The second objective was to evaluate how  $\lambda_c$  values generated by our approach affected predictions of  $K_s$  from infiltration experiments. Here we used four different models to estimate  $K_s$  from steady-state infiltration, and then compared those results with both reference values and with those estimated using constant and soil-dependent  $\lambda_c$  values.

## 2. Theory

For water infiltrating into an unsaturated soil from a constant head source, the soil matric flux potential,  $\phi_m$  ( $L^2 T^{-1}$ ), is defined as (Gardner, 1958):

$$\phi_m = \int_{h_i}^{h_0} K(h) dh \quad h_i \leq h \leq h_0 \quad (1a)$$

where  $K$  ( $L T^{-1}$ ) is hydraulic conductivity and  $h$  (L) is water pressure head, with an initial value  $h_i$  (L) and a source pressure head  $h_0$  (L). Eq. (1a) simplifies to Eq. (1b) when water infiltrates from a ponded source:

$$\phi_m = \int_{h_i}^0 K(h) dh \quad h_i \leq h \leq 0 \quad (1b)$$

The macroscopic capillary length,  $\lambda_c$  (L), is defined as (Philip, 1985; Smith et al., 2002):

$$\lambda_c = \frac{\phi_m}{\Delta K} \quad (2)$$

where  $\Delta K$  represents the difference between the saturated soil hydraulic conductivity,  $K_s$  ( $L T^{-1}$ ), and the initial soil hydraulic conductivity,  $K_i$  ( $L T^{-1}$ ), i.e.,  $\Delta K = K_s - K_i$ .

According to White and Sully (1987), Eq. (2) can be rewritten as:

$$\lambda_c = \frac{b S^2}{\Delta \theta \Delta K} \quad (3)$$

where  $b$  is a dimensionless constant dependent on the shape of the soil water diffusivity function,  $S$  ( $L T^{-0.5}$ ) is the soil sorptivity (Philip, 1957),  $\Delta \theta$  stands for the difference between the saturated,  $\theta_s$  ( $L^3 L^{-3}$ ), and initial,  $\theta_i$  ( $L^3 L^{-3}$ ), volumetric soil water contents, i.e.,  $\Delta \theta = \theta_s - \theta_i$ . For field soils,  $b$  is commonly set equal to 0.55 even though it can theoretically vary from 1/2 to  $\pi/4$  (White and Sully, 1987).  $K_i$  is often assumed negligible, such that  $\Delta K = K_s$  (White and Sully, 1992).

Estimating  $\lambda_c$  with Eq. (3) requires prior determination of sorptivity and hydraulic conductivity. These quantities can be estimated thanks to water infiltration experiments and fitting to the quasi-exact implicit (QEI) model developed by Haverkamp et al. (1994) or its related approximate expansions (see Lassabatere et al., 2009 for more details). Haverkamp et al. (1994) proposed the following approximate expansion for the description of the steady-state for three-dimensional (3D) water infiltration from a disc source while maintaining a zero water pressure head at the soil surface:

$$I_{3D}^{+\infty}(t) = \left( K_s + \frac{\gamma S^2}{r \Delta \theta} \right) t + \frac{S^2}{2(1-\beta) \Delta K} \ln \left( \frac{1}{\beta} \right) \quad (4)$$

where  $r$  (L) is the radius of the source, and  $\gamma$  and  $\beta$  are two infiltration constants, often fixed at  $\gamma = 0.75$  and  $\beta = 0.6$  (Haverkamp et al., 1994). Eq. (4) was later extended to include infiltration experiments from cylindrical sources with a slightly ponded water source (Ross et al., 1996) with negligible effect on results.

Eq. (4) is a linear equation of the form:

$$I_{3D}^{+\infty}(t) = i_s t + b_s \quad (5)$$

with  $b_s$  (L) and  $i_s$  ( $L T^{-1}$ ) defined as functions of hydraulic conductivity and sorptivity as follows:

$$i_s = K_s + \frac{\gamma S^2}{r \Delta \theta} \quad (6a)$$

$$b_s = \frac{S^2}{2(1-\beta) \Delta K} \ln \left( \frac{1}{\beta} \right) \quad (6b)$$

In this study, we use Eq. (6b) to quantify the ratio between sorptivity and the difference in hydraulic conductivity, as previously suggested by Castellini et al. (2018):

$$\frac{S^2}{\Delta K} = \frac{b_s}{c} \quad (7a)$$

$$C = \frac{1}{2(1-\beta)} \ln \left( \frac{1}{\beta} \right) \quad (7b)$$

Eqs. (3) and (7) can be combined to explicitly solve for  $\lambda_c$ :

$$\lambda_c = \frac{b S^2}{\Delta \theta \Delta K} = \frac{b}{\Delta \theta} \frac{b_s}{c} \quad (8a)$$

$$\lambda_c = \frac{b}{\frac{1}{2(1-\beta)} \ln \left( \frac{1}{\beta} \right) \Delta \theta} \frac{b_s}{\Delta \theta} \quad (8b)$$

Under the common assumptions that  $b = 0.55$  and  $\beta = 0.6$ , Eq. (8b) can be simplified as follows:

$$\lambda_c = 0.861 \frac{b_s}{\Delta \theta} \quad (9)$$

Eq. (9) constitutes a considerable simplification, as  $\lambda_c$  can now be estimated by only using the steady-state infiltration data (to determine  $b_s$ ) and a measurement of the initial and saturated soil water contents,  $\theta_i$  and  $\theta_s$ . Indeed,  $b_s$  is calculated as the intercept of the linear regression fitted to the steady-state portion of the experimental infiltration curve (Eq. 5), so  $b_s$  calculation does not require the use of Eq. (6b). Note that the simplified proposed method combines equations related to two approaches with distinct, but not necessarily incompatible, assumptions. The first approach by White and Sully (1987) was originally developed assuming the Gardner (1958) model for the hydraulic conductivity function. The second approach developed by Haverkamp et al. (1994) and Smettem et al. (1994) does not expect any specific hydraulic functions, but requires that these functions follow a specific equation defining the infiltration constant  $\beta$  (equation 6 in Haverkamp et al., 1994).

Eq. (9) may also simplify and improve estimates for  $K_s$ , as  $\lambda_c$  is an important and often unknown parameter in many infiltration models. Four examples of methods that require  $\lambda_c$  to estimate  $K_s$  from steady-state infiltration data include:

- i) the One-Ponding Depth (OPD) method by Reynolds and Elrick (1990)

$$K_s = \frac{\frac{i_s \pi r^2}{\lambda_c} (0.316 \frac{d}{r} + 0.184)}{r \left( \frac{H}{\lambda_c} + 1 \right) + \left( 0.316 \frac{d}{r} + 0.184 \right) \frac{\pi r^2}{\lambda_c}} \quad (10)$$

**Table 2.** Soil hydraulic parameters for the five studied soils used to model the infiltration experiments, originally from Carsel and Parrish (1988).

Soil texture	Sand	Loamy Sand	Sandy Loam	Loam	Silt Loam	Silty Clay Loam
$\theta_r$	0.045	0.057	0.065	0.078	0.067	0.089
$\theta_s$	0.43	0.41	0.41	0.43	0.45	0.43
$\alpha_{vc}$ (mm <sup>-1</sup> )	0.0145	0.0124	0.0075	0.0036	0.002	0.001
$n$	2.68	2.28	1.89	1.56	1.41	1.23
$K_s$ (mm h <sup>-1</sup> )	297.0	145.9	44.2	10.44	4.5	0.7
$l$	0.5	0.5	0.5	0.5	0.5	0.5

**ii) Method 2 by Wu et al. (1999) (WU2)**

$$K_s = \frac{i_s}{0.9084 \left( \frac{H+\lambda_c}{G^*} + 1 \right)} \quad (11)$$

**iii) the Steady version of the Simplified method based on a Beerkan Infiltration run (SSBI) by Bagarello et al. (2017)**

$$K_s = \frac{i_s}{\frac{\gamma_w \lambda_c}{r} + 1} \quad (12)$$

**iv) Approach 4 (A4) by Stewart and Abou Najm (2018b)**

$$K_s = \frac{i_s}{\left( \frac{H+\lambda_c}{G^*} + 1 \right)} \quad (13)$$

where  $d$  (L) is the ring insertion depth into the soil,  $r$  (L) is the ring radius,  $G^* = d + r/2$ ,  $H$  (L) is the ponding depth of water, and  $\gamma_w$  is a dimensionless constant related to the shape of the wetting front (White and Sully, 1987).  $\gamma$ , the infiltration constant defined above, was set equal to 0.75 (Smettem et al., 1994) and  $\gamma_w$  was set equal to 1.818, as suggested by Reynolds and Elrick (2002).

**3. Material and methods****3.1. Analytically generated data**

We assessed the accuracy of the proposed calculation approach for  $\lambda_c$  and  $K_s$  by using the same six soils considered by Hinnell et al. (2009) and Bagarello et al. (2017): sand, loamy sand, sandy loam, loam, silt loam, silty clay loam. These soils were chosen to cover a wide range of hydraulic responses. We modelled the infiltration experiments for these synthetic soils using the infiltration model proposed by Smettem et al. (1994):

$$I(t) = I_{1D}(t) + \frac{\gamma S^2}{r_d \Delta \theta} \quad (14)$$

where  $I$  (L) is 3D cumulative infiltration and  $I_{1D}$  (L) is the 1D cumulative infiltration into an uniform, initially unsaturated soil profile, which can be modelled by the following implicit equation (Haverkamp et al., 1990):

$$\frac{2\Delta K^2}{S^2} t = \frac{1}{1-\beta} \left[ \frac{2\Delta K}{S^2} (I_{1D}(t) - K_i t) - \ln \left( \frac{\exp(2\beta \frac{\Delta K}{S^2} (I_{1D}(t) - K_i t) + \beta - 1)}{\beta} \right) \right] \quad (15)$$

To also test the effect of the initial soil water content on parameters predictions, initial values of  $Se$ , ranging from 0.1 to 0.8 were converted to equivalent  $\theta_i$  values for each soil using the relationship  $Se = (\theta_i - \theta_r)/(\theta_s - \theta_r)$ , with  $\theta_r$  (L<sup>3</sup> L<sup>-3</sup>) representing the residual water content. The sorptivity was then estimated as follows (Parlange, 1975):

$$S = \sqrt{\int_{\theta(\theta_i)}^0 (\theta_s + \theta - 2\theta_i) K(h) dh} \quad (16)$$

The integrals in Eqs. (16) and (1b) were computed using the intg function defined in Scilab (Campbell et al., 2010). The water

retention curve and the hydraulic conductivity functions were calculated according to the van Genuchten–Mualem model (Mualem, 1976; van Genuchten, 1980):

$$Se = \left[ \frac{1}{1 + (\alpha_{vc} |h|)^n} \right]^m \quad (17a)$$

$$m = 1 - \frac{1}{n} \quad (17b)$$

$$K(Se) = K_s Se^l \left[ 1 - (1 - Se^{1/m})^m \right]^2 \quad (17c)$$

where  $\alpha_{vc}$  (L<sup>-1</sup>) is an empirical parameter related to the water pressure head,  $n$  is the pore size distribution index, and  $l$  is the pore connectivity parameter, which we assumed to be 0.5 following Mualem (1976). Hydraulic parameters for the six synthetic soils were taken from Carsel and Parrish (1988), with  $K_s$  values reported in that text used to represent the reference saturated hydraulic conductivity (Table 2). Default values of  $\beta = 0.6$  and  $\gamma = 0.75$  were assumed, as commonly suggested by many investigations (Angulo-Jaramillo et al., 2019).

To ensure steady-state conditions, each infiltration process was modelled for a period three times longer than the maximum time for which the explicit short-term expansion of Eq. (15) (Haverkamp et al., 1994) is considered valid, with  $t_{max}$  (T) calculated as follows (Lassabatere et al., 2006):

$$t_{max} = \frac{1}{4(1-\beta)^2} \left( \frac{S}{K_s} \right)^2 \quad (18a)$$

$$B = \frac{2-\beta}{3} \left( 1 - \frac{K_i}{K_s} \right) + \frac{K_i}{K_s} \quad (18b)$$

These analytical data were used to estimate the intercept,  $b_s$  (L), and the slope,  $i_s$  (L T<sup>-1</sup>), by linear regression analysis of the last three data points of the cumulative infiltration time series. Then, we defined the estimator for  $\lambda_c$ ,  $\hat{\lambda}_c$ , using Eq. (9) and the estimator for  $K_s$ ,  $\hat{K}_s$ , via the standard predictive equations for  $K_s$  (Eqs. 10-13).

The reference macroscopic capillary length,  $\lambda_c$ , was calculated for each combination of soil type and initial  $Se$  value using Eq. (2). Relative error,  $Er$ , was then calculated for each estimated value for  $\hat{\lambda}_c$  and  $\hat{K}_s$  compared to the corresponding reference value (i.e.,  $\lambda_c$  and  $K_s$ ) as follows:

$$Er(x) = 100 \times \frac{\hat{x} - x}{x} \quad (19)$$

where  $\hat{x}$  is the estimated value and  $x$  is the target, i.e., the reference value  $\lambda_c$  (Eq. 2) or  $K_s$  (Table 2). According to the accuracy criterion by Reynolds (2013), the estimates were deemed accurate when they fell within the range  $0.75 \leq \hat{x}/x \leq 1.25$  (i.e.  $\leq 25\%$  error). This stringent criterion was used because the parameters were estimated by analytically generated data, and therefore were free of the perturbations embedded in field and laboratory measurements (e.g., measurement error, random noise and natural variability).



**Table 3.** Summary of the Beerkan infiltration database. Total number of Beerkan infiltration experiments ( $N_{tot}$ ) = 433.

Country	Site	$N$	$D$ (cm)	$V$ (mL)	Coordinates	Reference
Burundi	Nyamutobo (Ruyigi)	77	15	150	3°27'50" S, 30°15'40" E	Bagarello et al. (2011)
Burundi	Kinyami (Ngozi)	20	15	150	2°54'30" S, 29°49'06" E	
Italy	Giampilieri	11	15	150	38°4'8" N, 15°28'26" E	Bagarello et al. (2013)
Italy	Palermo - SAAF (Sicily)	8	30	800	38°6'25" N, 13°21'6" E	Bagarello et al. (2014b)
Italy	Caccamo (Sicily)	4	30	800	37°52'34" N, 13°38'43" E	
Italy	Corleone (Sicily)	20	30	800	37°48'35" N, 13°17'49" E	
Italy	Sparacia (Sicily)	8	30	800	37°38'11" N, 13°45'50" E	
Italy	Palermo - SAAF (Sicily)	10	8.5	64	38°6'25" N, 13°21'6" E	Bagarello et al. (2014a)
Italy	Sparacia (Sicily)	10	8.5	64	37°38'10" N, 13°45'59" E	
Italy	Palermo - Parco d'Orleans (Sicily)	10	8.5	64	38°6'26" N, 13°20'59" E	
Italy	Villabate (Sicily)	10	8.5	64	38°4'53" N, 13°25'7" E	
Italy	Palermo - SAAF (Sicily)	12	15	200	38°6'25" N, 13°21'6" E	Bagarello et al. (2014c)
Italy	Palermo - SAAF (Sicily)	4	30	800	38°6'25" N, 13°21'6" E	
Italy	Pietranera (Sicily)	4	15	200	37°32'25" N, 13°30'44" E	
Italy	Pietranera (Sicily)	4	30	800	37°32'25" N, 13°30'44" E	
Italy	Caccamo (Sicily)	4	15	200	37°52'34" N, 13°38'43" E	
Italy	Corleone (Sicily)	20	15	200	37°48'35" N, 13°17'49" E	
Italy	Sparacia (Sicily)	8	15	200	37°38'11" N, 13°45'50" E	
Burundi	Nyamutobo (Ruyigi)	75	15	150	3°27'50" S, 30°15'40" E	
Italy	Palermo - Parco d'Orleans (Sicily)	10	15	150	38°6'26" N, 13°20'59" E	Alagna et al. (2016)
Italy	Palermo - SAAF (Sicily)	10	15	150	38°6'25" N, 13°21'6" E	Di Prima et al. (2016)
Italy	Palermo - Parco d'Orleans (Sicily)	10	15	150	38°6'26" N, 13°20'59" E	
Italy	Sparacia (Sicily)	10	15	150	37°38'10" N, 13°45'59" E	
France	Crépieux-Charmy (Lyon)	9	15	150	45°47'42" N, 4°53'19" E	
Spain	Les Alcusses de Moixent (Valencia)	10	8.5	48	38°48'33" N, 0°49'3" O	Di Prima et al. (2017)
Italy	Palermo - SAAF (Sicily)	5	5	17	38°6'25" N, 13°21'6" E	Di Prima et al. (2018a)
Italy	Palermo - Parco d'Orleans (Sicily)	5	5	17	38°6'26" N, 13°20'59" E	
Italy	Sparacia (Sicily)	5	5	17	37°38'10" N, 13°45'59" E	
Italy	Baratz Lake watershed (Sardinia)	40	8	43	40°41'53" N, 8°14'4" E	Di Prima et al. (2018b)

<sup>†</sup> Department of Agricultural, Food and Forest Sciences (SAAF = Scienze Agrarie, Alimentari e Forestali).

$N$  = Number of Beerkan infiltration experiments;  $D$  (cm) = ring diameter;  $V$  (mL) = water volume applied with each pouring.

### 3.2. The Beerkan infiltration database

In this investigation we also considered a large database of single ring (Beerkan) infiltration experiments carried out in four different countries, Italy, Burundi, France and Spain, during the period 2010-2017 (Table 3). Nearly half of the runs were carried out in Sicily, Italy (202 out of 433), and another ~1/3 of the runs (152 out of 433) were carried out in Burundi in the African Great Lakes region. The tested soils covered a range of textures, from sandy to clayey (Figure 1).

The Beerkan experiment is a variation of the single-ring infiltrometer technique, which consists of infiltrating water through a ring inserted shallowly (e.g., 1 cm) into the soil with a quasi-zero head of water imposed on the soil surface (Braud et al., 2005). All Beerkan experiments were carried out according to the methodology described by Lassabatere et al. (2006). First, a stainless steel ring was inserted shallowly into the soil (~1 cm). Then, water was poured on the confined soil surface in fixed volume increments ( $V$ ) to establish and maintain ponding conditions. The increments,  $V$ , ranged from 17 to 800 mL depending on ring diameter (Table 3). The energy of the falling water was dissipated with fingers to minimize the soil disturbance owing to water pouring, as commonly suggested (e.g., Di Prima et al., 2019). For each poured volume, the time needed for the water to infiltrate was recorded. The total number of poured volumes varied depending on time needed to reach steady state, as required by the Beerkan method (Angulo-Jaramillo et al., 2019).

We then estimated the intercept,  $b_s$  (mm), and the slope,  $i_s$  (mm h<sup>-1</sup>), of the regression line fitted to the cumulative

infiltration time series. The final three data points were used, as those were assumed to represent steady state infiltration conditions. We estimated  $K_s$  by using Eqs. (10-13) and constraining  $\lambda_c$  through three different approaches:

- **Scenario 1:** determining  $\lambda_c$  through Eq. (9);
- **Scenario 2:** using  $\lambda_c = 83$  mm, taking into account that it represents the suggested first approximation value for most field soils (Elrick and Reynolds, 1992);
- **Scenario 3:** using a soil-dependent  $\lambda_c$  value according to Table 1. Specifically, we used  $\lambda_c = 250$  mm for soils with sand content < 20%, 83 mm for sand contents between 20 and 70%, and 28 mm when the soil had > 70% sand (Bagarello et al., 2017).

For the experimental dataset, the comparison of the estimator to the target is not possible. Indeed, we don't have any information on the real value of the macroscopic capillary length, given that previously developed methods to estimate  $\lambda_c$  have all presented some limitations, as discussed in the Introduction. Instead, we compared the estimates to representative values from the five soil capillarity categories suggested by Elrick and Reynolds (1992). Note that these categories were originally proposed to select a representative value for five soil texture-structure categories (Table 1) when calculating  $K_s$  by the OPD method (Angulo-Jaramillo et al., 2016). In this investigation, we also proposed range of values for each category as detailed in Table 1. The range values of the intermediate categories (strong, moderate and weak) were

**Table 4.** Summary of the soil hydraulic properties for the six synthetic soils.

Soil	$S_e$	$h_i$ (mm)	$\theta_i$ ( $\text{m}^3\text{m}^{-3}$ )	$S$ ( $\text{mm h}^{-0.5}$ ) (Eq. 16)	$\phi$ ( $\text{mm}^2 \text{h}^{-1}$ ) (Eq. 1b)	$\lambda_c$ (mm) (Eq. 2)	$\hat{\lambda}_c$ (mm) (Eq. 9)	$i_s$ ( $\text{mm h}^{-1}$ )	$b_s$ (mm)	$\hat{K}_s$ ( $\text{mm h}^{-1}$ )			
										OPD (Eq. 10)	WU2 (Eq. 11)	SSBI (Eq. 12)	A4 (Eq. 13)
Sand	0.1	269.0	0.083	86.5	11308.6	38.1	37.2	516.7	15.0	304.3	319.1	341.3	289.8
	0.2	174.5	0.122	81.3	11298.6	38.0	37.0	515.3	13.2	304.2	319.0	341.0	289.7
	0.3	133.1	0.160	75.7	11268.5	37.9	36.8	513.3	11.5	303.7	318.5	340.3	289.3
	0.4	107.8	0.199	69.6	11202.4	37.7	36.7	510.6	9.8	302.4	317.2	338.8	288.1
	0.5	89.7	0.237	62.9	11076.7	37.3	36.7	506.5	8.2	299.8	314.4	335.9	285.6
	0.6	75.2	0.276	55.5	10854.0	36.5	37.1	500.4	6.6	294.9	309.2	330.7	280.9
	0.7	62.5	0.314	46.9	10467.3	35.2	38.2	491.1	5.1	286.1	299.8	321.6	272.3
	0.8	50.2	0.353	36.8	9776.1	32.9	40.5	476.0	3.6	270.3	282.7	305.4	256.8
Loamy Sand	0.1	483.8	0.092	58.2	5602.2	38.4	37.4	254.5	13.8	149.5	156.7	167.8	142.4
	0.2	276.4	0.128	54.7	5598.0	38.4	37.2	253.8	12.2	149.5	156.7	167.6	142.4
	0.3	195.6	0.163	50.9	5584.2	38.3	36.9	252.8	10.6	149.3	156.6	167.4	142.3
	0.4	150.0	0.198	46.8	5552.5	38.1	36.6	251.4	9.0	149.0	156.2	166.9	141.9
	0.5	119.2	0.233	42.3	5490.2	37.6	36.4	249.3	7.5	148.1	155.4	165.8	141.2
	0.6	95.9	0.269	37.3	5376.9	36.9	36.3	246.1	6.0	146.4	153.6	163.9	139.5
	0.7	76.5	0.304	31.5	5176.0	35.5	36.5	241.3	4.5	143.2	150.2	160.4	136.5
	0.8	58.9	0.339	24.6	4811.2	33.0	37.4	233.4	3.1	137.2	143.8	153.9	130.6
Sandy Loam	0.1	1765.2	0.100	36.0	2145.5	49.7	48.3	86.5	17.4	45.4	47.2	52.1	42.9
	0.2	799.2	0.134	33.8	2145.5	49.7	48.0	86.3	15.4	45.4	47.2	52.0	42.9
	0.3	494.2	0.169	31.5	2140.3	49.5	47.6	85.9	13.4	45.4	47.2	52.0	42.9
	0.4	344.1	0.203	29.0	2129.8	49.3	47.1	85.3	11.3	45.3	47.2	51.8	42.9
	0.5	253.1	0.238	26.2	2107.9	48.8	46.5	84.5	9.3	45.2	47.0	51.6	42.7
	0.6	190.3	0.272	23.1	2066.0	47.8	45.7	83.3	7.3	44.8	46.7	51.2	42.5
	0.7	142.4	0.307	19.5	1988.8	46.0	44.9	81.4	5.4	44.2	46.1	50.3	41.8
	0.8	102.3	0.341	15.2	1843.8	42.7	44.0	78.1	3.5	42.8	44.6	48.7	40.6
Loam	0.1	16941.8	0.113	20.9	719.7	69.2	67.6	24.3	24.9	10.7	11.0	12.6	10.0
	0.2	4883.1	0.148	19.6	719.6	69.2	67.2	24.2	22.0	10.7	11.0	12.6	10.0
	0.3	2330.8	0.184	18.3	718.8	69.1	66.6	24.1	19.1	10.7	11.0	12.6	10.0
	0.4	1354.4	0.219	16.8	716.5	68.9	65.9	23.9	16.2	10.7	11.0	12.6	10.0
	0.5	866.2	0.254	15.2	711.0	68.4	64.8	23.7	13.2	10.7	11.0	12.6	10.0
	0.6	579.6	0.289	13.4	699.3	67.2	63.2	23.3	10.3	10.7	11.0	12.5	10.0
	0.7	390.5	0.324	11.3	676.0	65.0	61.0	22.7	7.5	10.6	10.9	12.4	9.9
	0.8	252.5	0.360	8.8	629.2	60.5	57.7	21.6	4.7	10.4	10.8	12.1	9.8
Silt Loam	0.1	$1.4 \times 10^5$	0.105	16.3	402.8	89.5	87.8	12.3	35.1	4.6	4.7	5.6	4.3
	0.2	25267.3	0.144	15.3	402.8	89.5	87.3	12.2	31.1	4.6	4.7	5.6	4.3
	0.3	9318.5	0.182	14.3	402.6	89.5	86.6	12.2	27.0	4.6	4.7	5.6	4.3
	0.4	4529.8	0.220	13.2	401.8	89.3	85.7	12.1	22.9	4.6	4.7	5.6	4.3
	0.5	2531.6	0.258	11.9	399.6	88.8	84.4	12.0	18.8	4.6	4.7	5.6	4.3
	0.6	1519.5	0.297	10.5	394.4	87.6	82.4	11.8	14.7	4.6	4.7	5.6	4.3
	0.7	933.0	0.335	8.9	383.2	85.2	79.3	11.5	10.6	4.6	4.7	5.5	4.3
	0.8	553.5	0.373	7.0	359.1	79.8	74.2	10.9	6.6	4.6	4.7	5.4	4.3
Silty Clay Loam	0.1	$2.2 \times 10^7$	0.123	6.0	60.0	85.7	84.9	1.9	30.3	0.7	0.7	0.9	0.7
	0.2	$1.1 \times 10^6$	0.157	5.6	60.0	85.7	84.5	1.9	26.8	0.7	0.7	0.9	0.7
	0.3	$1.9 \times 10^5$	0.191	5.2	60.0	85.7	84.1	1.9	23.3	0.7	0.7	0.9	0.7
	0.4	53399.3	0.225	4.8	60.0	85.7	83.4	1.9	19.8	0.7	0.7	0.9	0.7
	0.5	19954.8	0.259	4.4	59.9	85.5	82.5	1.8	16.3	0.7	0.7	0.9	0.7
	0.6	8725.5	0.294	3.9	59.5	85.0	81.0	1.8	12.8	0.7	0.7	0.9	0.7
	0.7	4137.5	0.328	3.3	58.5	83.6	78.5	1.8	9.3	0.7	0.7	0.9	0.7
	0.8	1966.9	0.362	2.6	55.9	79.9	73.6	1.7	5.8	0.7	0.7	0.9	0.7

calculated as the mean of the representative values of two consecutive categories.

The same issue arises for the estimation of the saturated hydraulic conductivity. In this case, we chose to use the BEST-steady method proposed by Bagarello et al. (2014a) as a benchmark, as an independent  $K_s$  datum that can be used for assessing simplified procedures or validating newly developed methods. This method estimates  $K_s$  as follows:

$$K_{s,BEST} = \frac{C i_s}{A b_s + C} \quad (20a)$$

$$A = \frac{y}{r(\theta_s - \theta_i)} \quad (20b)$$

Note that we also chose the Bagarello et al. (2014a) method because it requires the same experimental information as the  $\lambda_c$ -dependent methods considered in this investigation for estimating  $K_s$ , yet does not require an estimate of  $\lambda_c$ . We also avoided using laboratory measurements as benchmark, as they can induce experimental artifacts, such as soil compaction and

samples biased by pores, that may limit their comparability with in-situ measurements (Haverkamp et al., 1999).

To compare  $K_s$  values estimated by Eqs. (10-13) with the reference  $K_{s,BEST}$  values obtained by Eq. (20), we again used the relative error metric (Eq. 19). We also calculated paired differences for each method, i.e.,  $K_{s,BEST} - K_s$  and checked them for normality using the Kolmogorov-Smirnov test. For non-normally distributed data we used the Wilcoxon signed rank test to evaluate the median difference between paired observations at the 95% confidence level. All statistical analyses were carried out using the Minitab© computer program (Minitab Inc., State College, PA, USA).

## 4. Results

### 4.1. Analytical validation

#### 4.1.1. Estimating $\lambda_c$ from analytically generated data

When applied to the six synthetic soils, Eq. (2) yielded the highest  $\lambda_c$  values for fine-textured soils (Table 4). This is logical, since for fine soils the capillary contribution to water flow was

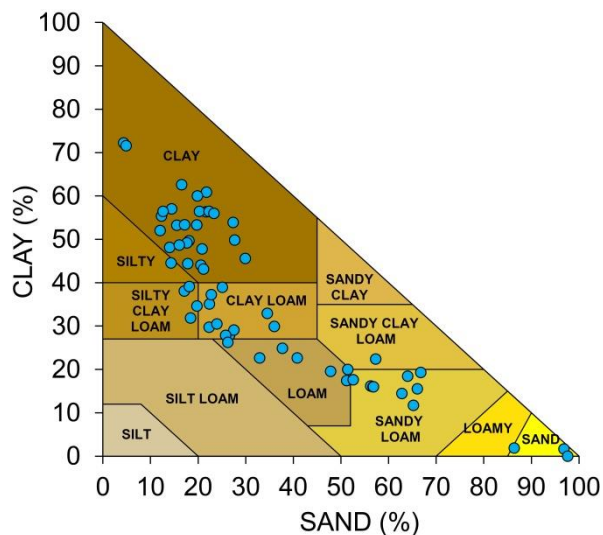


Figure 1. Textural classification of the soils included in the Beerkan infiltration database.

higher than for coarser soils. More specifically, high  $\lambda_c$  values were associated to initially flat  $K(h)$  relationships, i.e., when a decrease in pressure head determined a moderate pore emptying (Angulo-Jaramillo et al., 2016; Reynolds, 1994). Moreover,  $\lambda_c$  values decreased for all soils as  $Se$  increased.

When cumulative infiltration was calculated for all synthetic soils (Table 2) using Eqs. (14) and (15), all curves exhibited a typical concave shape as a function of time (Figure 2). As the process approached steady state, cumulative infiltration curves became approximately linear with time. This behaviour shows how the influence of capillarity decreases as the wetting front moves away from the source and the hydraulic gradient decreases (Xu et al., 2012). Note that the duration of the infiltration process decreased for higher values of  $Se$ , as steady-state conditions were attained in less time. In these cases, capillary forces only influenced infiltration during the early stage of the process.

The value of the linear regression model intercept,  $b_s$ , estimated from each curve was used in conjunction with the known  $\theta_i$  and  $\theta_s$  values to calculate  $\lambda_c$  using Eq. (9). Both  $b_s$  and

$i_s$  decreased in all soils as  $Se$  increased.  $b_s$  ranged from 3.1 to 35.1 mm, with larger values corresponding to the fine-textured silt loam and silty clay loam soils (Table 4). The slope of the linear regression model  $i_s$  had values as low as 1.7 mm h<sup>-1</sup> (fine soil) and as high as 516.7 mm h<sup>-1</sup> (coarse soil)

The estimated  $\hat{\lambda}_c$  for the six synthetic soils ranged from 36.3 to 87.8 mm, and were classified only into weak or moderate capillary categories (Table 1), although those soils had textures which ranged from sand to silty clay loam. Relative error,  $Er(\lambda_c)$ , between estimated  $\hat{\lambda}_c$  and reference  $\lambda_c$  values ranged from -7.9 to 23.3%, indicating that all  $\lambda_c$  values were accurate based on our stated criterion. The largest  $Er(\lambda_c)$  values were obtained for the coarse-textured sandy and loamy sand soils under initial wet conditions (Figure 3). Indeed, neglecting  $K_i$  is expected to introduce more uncertainty on  $\lambda_c$  estimations for higher  $Se$  values. Nevertheless,  $\lambda_c$  estimates were sufficiently accurate also in these cases, with error always < 25%.

#### 4.1.2. Estimating $K_s$ from analytically generated data

The values of the slope,  $i_s$ , estimated from the analytically generated curves were used to calculate  $K_s$  by the four  $\lambda_c$ -dependent methods, i.e., OPD (Eq. 10), WU2 (Eq. 11), SSBI (Eq. 12), A4 (Eq. 13). Then, relative error,  $Er(K_s)$ , was calculated using Eq. (14) (Figure 4).  $Er(K_s)$  ranged from -9.5 to 3.1% for OPD, from -5.4 to 7.4% for WU2, from 2.2 to 24.7% for SSBI, and from -14 to -2.4 % for A4. While we observe higher  $|Er(\lambda_c)|$  values for initial wet conditions (Figure 3), for  $K_s$ , we observe similar trends between the four methods but also a consistent vertical shift of the  $Er(K_s)$  values. For instance, for the SSBI method, lower errors corresponded to higher  $Se$  values. Conversely, for the A4 method, the errors always increased for increasing  $Se$  values, given that this method always underestimated  $K_s$ . We therefore argue that the discrepancies between the four methods were more relevant than the variations within a specific method due to different initial saturation degree. Nevertheless, the four methods always yielded  $K_s$  estimates close to the reference values, since  $|Er(K_s)|$  values were always < 25%. Mean  $|Er(K_s)|$  values were ordered

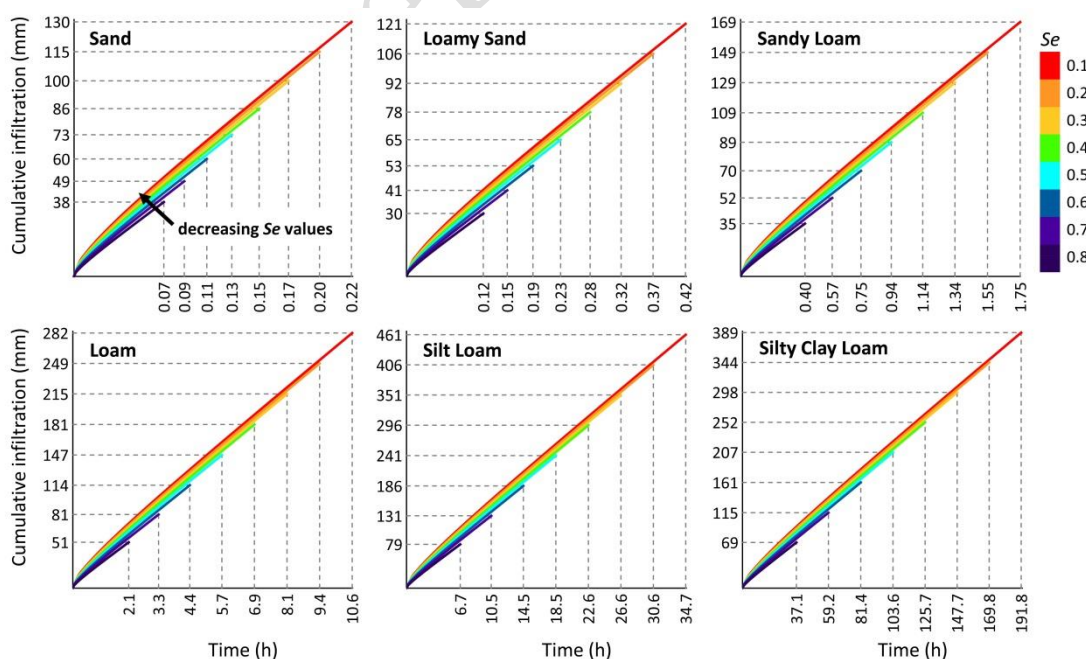
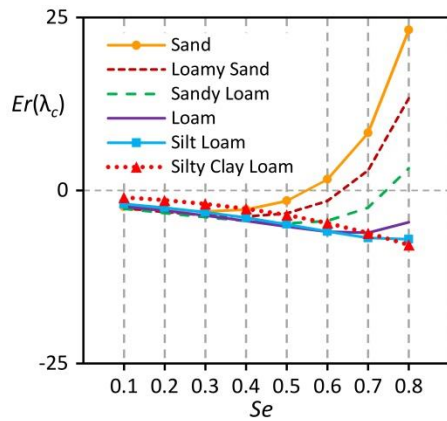


Figure 2. Cumulative infiltration curves for different soils and initial effective saturation degrees,  $Se$ . The curves were generated analytically using Eqs. (14) and (15) and the parameters listed in Table 2. The labels in ordinate and abscissa report respectively the total infiltrated water and the duration of the infiltration process. Note that the duration was fixed at three times the maximum time ( $t_{max}$ ) for which the explicit transient infiltration model proposed by Haverkamp et al. (1994) is valid.





**Figure 3.** Relative error,  $Er(\lambda_c)$ , of the estimated macroscopic capillary length compared to reference values for six synthetic soils listed in Table 2.

as  $OPD < A4 < WU2 < SSBI$ , showing that the OPD method yielded the lower  $|Er(K_s)|$  values.

## 4.2. Field testing

### 4.2.1. Estimating $\lambda_c$ from the Beerkan infiltration database

Eq. (9) was also used to estimate  $\lambda_c$  from the field-based single ring (Beerkan) infiltration experiments. The procedure worked for nearly all Beerkan tests; however, six of the tests had infiltration rates that increased with time (i.e., the cumulative infiltration curves exhibited convex shapes). Fitting Eq. (5) to those data yielded negative value for the intercept,  $b_s$ , which led to negative values for  $\lambda_c$ , which is meaningless from a physical point of view. Those six cases – two at the Kinyami site, one at the Palermo – SAAF site, and three at the Crépieux-Charmy site – were excluded from subsequent analysis. The remaining 427 successful tests yielded  $\lambda_c$  values ranging from 1.5 to 737.7 mm (Table 5), thus covering the full range of soil capillarity categories suggested by Elrick and Reynolds (1992) (Table 1).

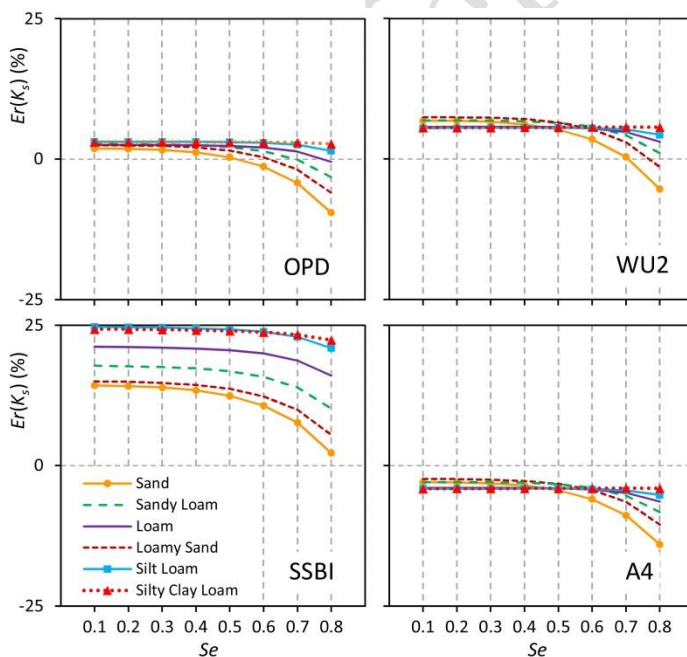


**Figure 4.** Relative error of the estimated values for saturated soil hydraulic conductivity,  $Er(K_s)$ , for six synthetic soils that were analyzed using four different methods. OPD = one-ponding depth (Eq. 10); WU2 = Method 2 (Eq. 11); SSBI = Steady version of the Simplified method based on a Beerkan Infiltration run (Eq. 12); A4 = Approach 4 (Eq. 13).

Across all soils, there was a consistent yet non-linear relationship between  $\lambda_c$  values and their corresponding intercepts  $b_s$  (Figure 5a). As shown by three different examples of  $\lambda_c$  estimation, cumulative infiltration shapes and times to steady-state conditions varied widely between soils with moderate (Figure 5b), strong (Figure 5c), and negligible capillarity (Figure 5d). In the first case (Figure 5b), cumulative infiltration exhibited the typical concave shape as a function of time. For this run, we estimated  $b_s$  value of 30.9 mm and a  $\lambda_c$  value of 49.2 mm (moderate capillarity). In the second case (Figure 5c), the cumulative infiltration curve exhibited a strong concave shape with a  $b_s$  value of 209.6 mm, yielding a  $\lambda_c$  value of 598.7 mm (strong capillarity). This behavior is typical for very fine soils, with low permeability. For this run, capillary forces predominated for almost the entire duration of the experiment. In the third case (Figure 5d), the cumulative infiltration curve had an almost linear shape with a  $b_s$  value of 1.0 mm, which translated to a  $\lambda_c$  value of 1.5 mm, i.e., lower than the considered threshold of 10 mm for negligible capillarity forces. This behaviour is typical for coarse-textured soils and occurs when the infiltration process is mainly driven by gravity. Altogether, 127 (29.7%) of the  $\lambda_c$  values represented strong capillarity conditions, 189 values (44.3%) represented moderate capillarity, 107 values (25.1%) represented weak capillarity, and 4 values (0.9%) represented negligible capillarity.

### 4.2.2. Estimating $K_s$ from the Beerkan infiltration database

The  $\lambda_c$  values determined through Eq. (9) were next used with four methods (i.e., OPD, WU2, SSBI, A4) to estimate  $K_s$  for the Beerkan dataset. The Wilcoxon signed rank test showed that all methods yielded  $K_s$  estimates significantly different from the BEST-steady values, and the differences between  $K_s$  and  $K_{s,BEST}$  were always non-normally distributed according to the Kolmogorov-Smirnov test. However, the discrepancies between

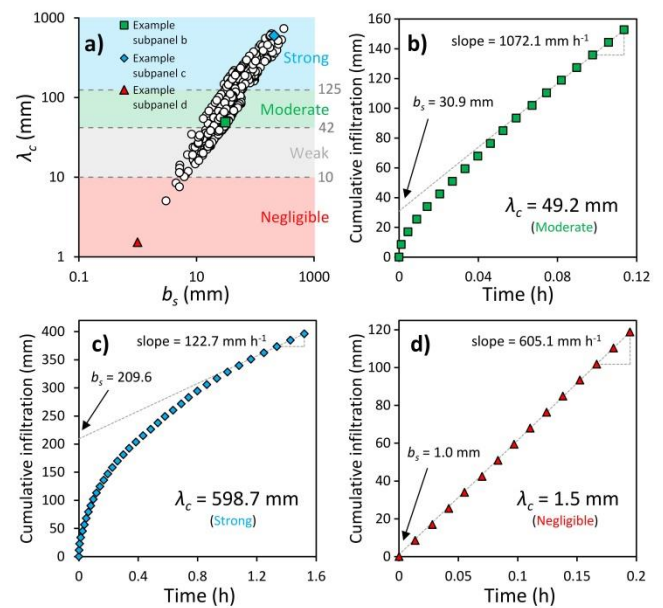


**Figure 5.** (a) Comparison between the estimated macroscopic capillary length,  $\lambda_c$ , and the intercept,  $b_s$ , of the regression line between cumulative infiltration and time under steady-state conditions. The soil capillarity categories are indicated by dashed horizontal lines. Also shown are examples of  $\lambda_c$  estimation for (b) moderate, (c) strong, and (d) negligible capillarity conditions.

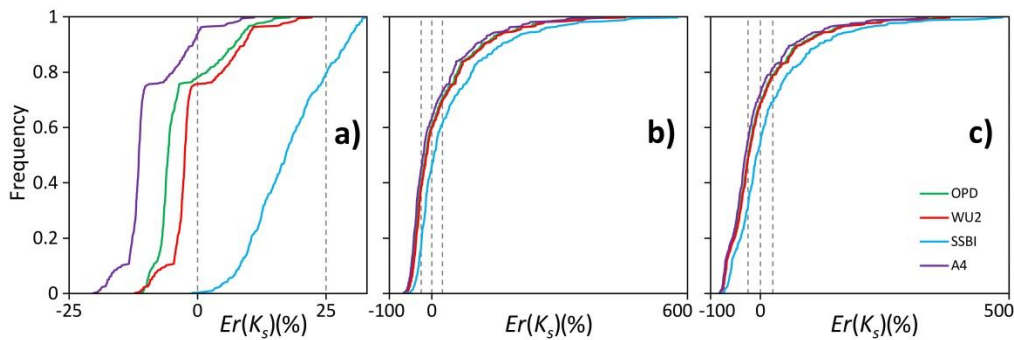


**Figure 6.** Cumulative empirical frequency distribution of relative error in estimated saturated hydraulic conductivity,  $Er(K_s)$ , when 427 experiments in the Beerkan database were analyzed with the four considered methods (i.e., OPD, WU2, SSBI, A4) and  $\lambda_c$  was constrained (a) using Eq. (9), (b) assuming  $\lambda_c = 83$  mm, (c) using a soil-dependent  $\lambda_c$  value. OPD = one-ponding depth (Eq. 10); WU2 = Method 2 (Eq. 11); SSBI = Steady version of the Simplified method based on a Beerkan Infiltration run (Eq. 12); A4 = Approach 4 (Eq. 13).

**Table 5.** Summary of the soil hydraulic properties estimated from the Beerkan database.

Statistic	$\lambda_c$ (mm) (Eq. 9)	$K_s$ (mm h <sup>-1</sup> )				
		BEST-steady (Eq. 20)	OPD (Eq. 10)	WU2 (Eq. 11)	SSBI (Eq. 12)	A4 (Eq. 13)
N	427	427	427	427	427	427
min	1.5	1.3	1.4	1.4	1.6	1.2
max	737.7	3550.9	3294.1	3493.8	3758.7	3173.7
mean	112.6	270.7	258.5	269.3	305.2	244.6
median	68.0	156.8	153.3	156.4	182.4	142.0
CV	101.3	142.0	140.1	141.3	137.6	141.3

methods were always  $\leq 25\%$ , with the exception of the SSBI method (Figure 6a). The WU2 method yielded the best overall fit with the BEST-steady values, with  $Er(K_s)$  values between -12.1 and 22.1%. The WU2 method yielded lower  $K_s$  estimates than the BEST-estimated values for 76% of the runs and higher  $K_s$  values for 24% of runs, and the median  $K_s$  values for the two methods differed by only a factor of 1.002. The OPD and A4 methods also performed well, though those methods tended to under-predict  $K_s$  to a greater extent than WU2, with 82% of OPD runs and 91% of A4 runs under-predicting  $K_s$ . The SSBI method, by contrast, yielded  $K_s$  values that were higher than  $K_{s,BEST}$  with only a single exception. The  $Er(K_s)$  values ranged from -1.0 to 32.8%, with 21% of the runs (88 out of 427) yielding higher values than the considered threshold of 25%.

Using constant (Scenario 2) or a soil-dependent (Scenario 3)  $\lambda_c$  values resulted in greater difference between  $K_s$  and  $K_{s,BEST}$ . With the constant  $\lambda_c$  value (Scenario 2),  $Er(K_s)$  values ranged from -66.8 to 576.9% (Figure 6b), with 68.4% of OPD runs, 68.1% of WU2 runs, 55.7% of SSBI runs and 72.1% of A4 runs yielding higher values than the considered threshold of 25%. With the soil-dependent  $\lambda_c$  values (Scenario 3),  $Er(K_s)$  values ranged from -82.9 to 486.5% (Figure 6c), with 70.5% of OPD runs, 69.3% of WU2 runs, 62.3% of SSBI runs and 74.0% of A4 runs yielding higher values than the considered threshold. These results also suggest that among the four considered methods, the SSBI was the least sensitive to the assumed  $\lambda_c$  value, with less runs (55.7 and 62.3% for scenario 2 and 3, respectively) yielding higher  $Er(K_s)$  values than the considered threshold of 25%.

## 5. Discussion

In this investigation, we developed a new procedure to estimate  $\lambda_c$  using simple Beerkan infiltration experiments and measurements of initial and saturated soil water contents (Eq. 9). Previous investigations also suggested that the measured infiltration curve contains the necessary information to estimate  $\lambda_c$  (e.g., Bagarello et al., 2014b, 2013; Stewart and Abou Najm, 2018a; Wu et al., 1999). However, those methods are based on

the analysis of the transient infiltration process and can be subject to considerable error, particularly due to uncertainties with the duration of the transient phase (Vandervaere et al., 2000). In contrast, the proposed method uses measurements collected during the steady-state stage of the infiltration process, where the infiltration rate ( $i_s$ ) is assumed to be independent of the initial infiltration phase (Bagarello et al., 2013). Estimating  $\lambda_c$  using the proposed method requires linear regression analysis of cumulative infiltration versus time to determine the intercept ( $b_s$ ). Because the magnitude of  $b_s$  depends on the entire cumulative infiltration curve (including the transient phase), that term is sensitive to the relative importance of capillary and gravity forces during ponded infiltration (Angulo-Jaramillo et al., 2019). Specifically, small  $b_s$  values indicate a linear infiltration curve, i.e., when gravity prevails over capillarity, which occurs primarily in coarse-textured and/or highly structured porous media. On the contrary, high intercept values indicate conditions when capillarity prevails over gravity, particularly in the transient infiltration phase, which occurs primarily in fine-textured soils. Therefore,  $b_s$  is expected to be a reliable predictor of the macroscopic capillary length, but one that necessitates collecting accurate data during the final stage of the infiltration process.

In this investigation, the proposed method (Eq. 9) was validated using both analytical and field data. The analytical verification demonstrated that Eq. (9) provided reliable  $\lambda_c$  estimates in nearly all conditions, including different soils and, for the same soils, under different initial soil water contents. For the field data, verification was conducted using a set of 427 Beerkan infiltration experiments carried out on different soils having a range of textural characteristics, i.e., from sandy to clayey. That analysis showed that nearly all soils (i.e., 99.1% of the experiments) yielded  $\lambda_c$  values falling within the realistic range  $10 \leq \lambda_c \leq 1000$  mm (Reynolds and Elrick, 2002); only four cases yielded  $\lambda_c$  values lower than 10 mm. Further, the proposed method predicted  $\hat{\lambda}_c$  values very close to the reference  $\lambda_c$  values, with all tests having relative errors between -23.2% and 7.9%. The consistency of Eq. (9) shows that it is a suitable method to constrain  $\lambda_c$ .

Many models to estimate  $K_s$  from field measurements (e.g., Eqs. 10-13), require knowledge of  $\lambda_c$ , which is often estimated based on general descriptions of soil textural and structural characteristics (e.g., Table 1). Previous research has shown that choosing an incorrect capillarity category can lead to threefold or greater error in estimated  $K_s$  (Bagarello et al., 2014b), and that  $K_s$  estimates are more sensitive to underpredictions of  $\lambda_c$



compared with overpredictions (Stewart and Abou Najm, 2018b). In this investigation we demonstrated that using constant or a soil-dependent  $\lambda_c$  value may result in considerably greater relative error when predicting  $K_s$ . Specifically, using Eq. (9) resulted in relative errors < 25% for all Beerkan tests when analyzed with three of the four methods, and < 30% when the fourth method was used. By comparison, assuming  $\lambda_c = 83$  mm resulted in relative error up to 600%, and using a soil-dependent  $\lambda_c$  value caused relative errors of close to 500%.

Beyond its use in estimating  $K_s$ ,  $\lambda_c$  can provide information on soil pore structure and water retention (Stewart and Abou Najm, 2018b), making it important to have a simple method for use in the field. For example, the proposed method for constraining  $\lambda_c$  may also facilitate the estimation of dynamic indicators, such as the flow-weighted mean pore radius and the number of hydraulically active pores per unit area previously proposed by Warrick and Broadbridge (1992) and Watson and Luxmoore (1986). The flow-weighted mean pore radius represents the size of pores that are actively conducting and it expresses the ability of a soil to transmit water (Reynolds and Elrick, 2005). These indicators, quantitatively linked to  $\lambda_c$  and  $K_s$ , are useful to understand the effects of land use and management on soil physical quality (Bouarafa et al., 2019; Castellini et al., 2019; Iovino et al., 2016). Therefore, accurate estimation of  $\lambda_c$  through Eq. (9) could also facilitate determination of dynamic indicators from infiltration experiments and improve soil quality assessment.

## 6. Summary and conclusions

In this investigation, we assessed a simple field method for estimating the macroscopic capillary length,  $\lambda_c$ , by only using a single-ring infiltration experiment of the Beerkan type and a measurement of the initial and saturated soil water contents. We validated the proposed method using both analytically generated data and a large database of 433 Beerkan infiltration experiments carried out in four countries (Italy, Burundi, France and Spain) over the period 2010–2017. The analytical validation supported our hypothesis that the intercept,  $b_s$ , is a reliable predictor of the macroscopic capillary length, while the testing carried out using the Beerkan database increased our confidence that the approach performs well under field conditions. Therefore, we conclude that the method proposed here constitutes an easy and effective solution for constraining  $\lambda_c$ , which at the same time can help users to better estimate  $K_s$  from field infiltration measurements. The proposed procedure may also avoid uncertainty due to an imprecise description of the transient state of infiltration, and any subjectivity caused by the selection of a representative  $\lambda_c$  value based solely on textural or structural characteristics.

## Funding

This work was supported through the INFILTRON Project (ANR-17-CE04-0010, Package for assessing infiltration & filtration functions of urban soils in stormwater management; <https://infiltron.org/>) funded by the French National Research Agency (ANR), and the “Programma Operativo Nazionale (PON) Ricerca e Innovazione 2014-2020 (Linea 1 - Mobilità dei ricercatori, AIM1853149, CUP: J54I18000120001) funded by the European Regional Development Fund (ERDF) and the Italian Ministry of Education, University and Research (MIUR).

## CRedit authorship contribution statement

**Simone Di Prima:** Conceptualization, Funding acquisition, Methodology, Writing - Original Draft, Formal analysis, Visualization, Writing - Review & Editing. **Ryan D. Stewart:** Methodology, Writing - Review & Editing. **Mirko Castellini:** Formal analysis, Writing - Review & Editing. **Vincenzo Bagarello:** Methodology, Writing - Review & Editing. **Majdi R. Abou Najm:** Formal analysis, Writing - Review & Editing. **Mario Pirastru:** Formal analysis, Writing - Review & Editing. **Filippo Giadrossich:** Formal analysis, Writing - Review & Editing. **Massimo Iovino:** Methodology, Writing - Review & Editing. **Rafael Angulo-Jaramillo:** Formal analysis, Writing - Review & Editing. **Laurent Lassabatere:** Funding acquisition, Methodology, Writing - Review & Editing.

## Author Contributions

SDP outlined the investigation and wrote the first draft of the manuscript. SDP, MI, VB, LL and RDS developed the theory. SDP, MAN, RAJ, FG, MP and MC planned the analytical validation and analyzed the field data. All authors contributed to discussing the results and developing the final version of the manuscript.

## Conflicts of interest

The authors declare that they have no known competing financial interests or personal relationships that could have appeared to influence the work reported in this paper.

## References

- Angulo-Jaramillo, R., Bagarello, V., Di Prima, S., Gosset, A., Iovino, M., Lassabatere, L., 2019. Beerkan Estimation of Soil Transfer parameters (BEST) across soils and scales. *Journal of Hydrology* 576, 239–261. <https://doi.org/10.1016/j.jhydrol.2019.06.007>
- Angulo-Jaramillo, R., Bagarello, V., Iovino, M., Lassabatere, L., 2016. Infiltration Measurements for Soil Hydraulic Characterization. Springer International Publishing.
- Bagarello, V., Castellini, M., Di Prima, S., Giordano, G., Iovino, M., 2013. Testing a Simplified Approach to Determine Field Saturated Soil Hydraulic Conductivity. *Procedia Environmental Sciences* 19, 599–608. <https://doi.org/10.1016/j.proenv.2013.06.068>
- Bagarello, V., Di Prima, S., Iovino, M., 2017. Estimating saturated soil hydraulic conductivity by the near steady-state phase of a Beerkan infiltration test. *Geoderma* 303, 70–77. <https://doi.org/10.1016/j.geoderma.2017.04.030>
- Bagarello, V., Di Prima, S., Iovino, M., 2014a. Comparing Alternative Algorithms to Analyze the Beerkan Infiltration Experiment. *Soil Science Society of America Journal* 78, 724. <https://doi.org/10.2136/sssaj2013.06.0231>
- Bagarello, V., Di Prima, S., Iovino, M., Provenzano, G., 2014b. Estimating field-saturated soil hydraulic conductivity by a simplified Beerkan infiltration experiment. *Hydrological Processes* 28, 1095–1103. <https://doi.org/10.1002/hyp.9649>
- Bagarello, V., Iovino, M., Elrick, D., 2004. A Simplified Falling-Head Technique for Rapid Determination of Field-Saturated Hydraulic Conductivity. *Soil Science Society of America Journal* 68, 66. <https://doi.org/10.2136/sssaj2004.6600>
- Bouarafa, S., Lassabatere, L., Lipeme-Kouyi, G., Angulo-Jaramillo, R., 2019. Hydrodynamic Characterization of Sustainable Urban Drainage Systems (SuDS) by Using Beerkan Infiltration Experiments. *Water* 11, 660. <https://doi.org/10.3390/w11040660>
- Bowen, H., 1964. Unsaturated Flow in Ground-Water Hydraulics. *Journal of the Hydraulics Division* 90, 121–144.
- Braud, I., De Condappa, D., Soria, J.M., Haverkamp, R., Angulo-Jaramillo, R., Galle, S., Vauclin, M., 2005. Use of scaled forms of the infiltration equation for the estimation of unsaturated soil hydraulic properties (the Beerkan method). *European Journal of Soil Science* 56, 361–374. <https://doi.org/10.1111/j.1365-2389.2004.00660.x>
- Campbell, S.L., Chancelier, J.-P., Nikoukhan, R., 2010. Modeling and Simulation in Scilab/Scicos with ScicosLab 4.4, 2nd ed. Springer-Verlag, New York.
- Carsel, R.F., Parrish, R.S., 1988. Developing joint probability distributions of soil water retention characteristics. *Water Resour. Res.* 24, 755–769. <https://doi.org/10.1029/WR024i005p00755>
- Castellini, M., Di Prima, S., Iovino, M., 2018. An assessment of the BEST procedure to estimate the soil water retention curve: A comparison with the evaporation method. *Geoderma* 320, 82–94. <https://doi.org/10.1016/j.geoderma.2018.01.014>
- Castellini, M., Fornaro, F., Garofalo, P., Giglio, L., Rinaldi, M., Ventrella, D., Vitti, C., Vonella, A.V., 2019. Effects of No-Tillage and Conventional Tillage on Physical and Hydraulic Properties of Fine Textured Soils under Winter Wheat. *Water* 11, 484. <https://doi.org/10.3390/w11030484>
- Di Prima, S., Castellini, M., Majdi R. Abou Najm, Stewart, R.D., Angulo-Jaramillo, R., Winiarski, T., Lassabatere, L., 2019. Experimental assessment of a new

- comprehensive model for single ring infiltration data. *Journal of Hydrology* 573, 937–951. <https://doi.org/10.1016/j.jhydrol.2019.03.077>
- Elrick, D.E., Reynolds, W.D., 1992. Methods for analyzing constant-head well permeameter data. *Soil Science Society of America Journal* 56, 320. <https://doi.org/10.2136/sssaj1992.03615995005600010052x>
- Gardner, W., 1958. Some steady-state solutions of the unsaturated moisture flow equation with application to evaporation from a water table. *Soil science* 85, 228–232.
- Haverkamp, R., Bouraoui, F., Zammit, C., Angulo-Jaramillo, R., 1999. Soil properties and moisture movement in the unsaturated zone. *Handbook of groundwater engineering*.
- Haverkamp, R., Parlange, J.-Y., Starr, J., Schmitz, G., Fuentes, C., 1990. Infiltration under ponded conditions: 3. A predictive equation based on physical parameters. *Soil science* 149, 292–300. <https://doi.org/10.1097/00010694-199005000-00006>
- Haverkamp, R., Ross, P.J., Smettem, K.R.J., Parlange, J.Y., 1994. Three-dimensional analysis of infiltration from the disc infiltrometer: 2. Physically based infiltration equation. *Water Resour. Res.* 30, 2931–2935. <https://doi.org/10.1029/94WR01788>
- Hinnell, A.C., Lazarovitch, N., Warrick, A.W., 2009. Explicit infiltration function for boreholes under constant head conditions: INFILTRATION FUNCTION FOR BOREHOLES. *Water Resources Research* 45, n/a-n/a. <https://doi.org/10.1029/2008WR007685>
- Iovino, M., Castellini, M., Bagarello, V., Giordano, G., 2016. Using Static and Dynamic Indicators to Evaluate Soil Physical Quality in a Sicilian Area. *Land Degrad. Develop.* 27, 200–210. <https://doi.org/10.1002/ldr.2263>
- Kutilek, M., Nielsen, D.R., 1994. *Soil Hydrology*. CATENA VERLAG, Reiskirchen.
- Lassabatere, L., Angulo-Jaramillo, R., Soria Ugalde, J.M., Cuenca, R., Braud, I., Haverkamp, R., 2006. Beerkan estimation of soil transfer parameters through infiltration experiments—BEST. *Soil Science Society of America Journal* 70, 521. <https://doi.org/10.2136/sssaj2005.0026>
- Lassabatere, L., Angulo-Jaramillo, R., Soria-Ugalde, J.M., Šimůnek, J., Haverkamp, R., 2009. Numerical evaluation of a set of analytical infiltration equations: EVALUATION INFILTRATION. *Water Resources Research* 45, n/a-n/a. <https://doi.org/10.1029/2009WR007941>
- Mualem, Y., 1976. A new model for predicting the hydraulic conductivity of unsaturated porous media. *Water Resour. Res.* 12, 513–522.
- Nimmo, J.R., Schmidt, K.M., Perkins, K.S., Stock, J.D., 2009. Rapid Measurement of Field-Saturated Hydraulic Conductivity for Areal Characterization. *Vadose Zone Journal* 8, 142. <https://doi.org/10.2136/vzj2007.0159>
- Parlange, J.-Y., 1975. Convergence and validity of time expansion solutions: a comparison to exact and approximate solutions. *Soil Science Society of America Journal* 39, 3–6.
- Philip, J., 1957. The theory of infiltration: 4. Sorptivity and algebraic infiltration equations. *Soil sci* 84, 257–264.
- Philip, J.R., 1985. Reply To “Comments on Steady Infiltration from Spherical Cavities.” *Soil Science Society of America Journal* 49, 788–789. <https://doi.org/10.2136/sssaj1985.03615995004900030055x>
- Raats, P.A.C., 1976. Analytical Solutions of a Simplified Flow Equation. *Transactions of the ASAE* 19, 0683–0689. <https://doi.org/10.13031/2013.36096>
- Reynolds, W., Elrick, D., 2002. 3.4.3.2.b Pressure infiltrometer. In *Methods of Soil Analysis, Part 4, Physical Methods*, Dane JH, Topp GC (eds). SSSA Book Series, No. 5. Soil Sci. Soc. Am.: Madison, Wisconsin, USA 4, 826–836.
- Reynolds, W., Elrick, D., Youngs, E., 2002. 3.4.3.2 Ring or cylinder infiltrometers (vadose zone). In *Methods of Soil Analysis, Part 4, Physical Methods*, Dane JH, Topp GC (eds). SSSA Book Series, No. 5. Soil Sci. Soc. Am.: Madison, Wisconsin, USA 818–820.
- Reynolds, W.D., 2013. An assessment of borehole infiltration analyses for measuring field-saturated hydraulic conductivity in the vadose zone. *Engineering Geology* 159, 119–130. <https://doi.org/10.1016/j.enggeo.2013.02.006>
- Reynolds, W.D., 1994. Letter to the editor. Comment on “comparison of three methods for assessing soil hydraulic properties” by G. B. Paige and D. Hillel. *Soil Science* 157, 120.
- Reynolds, W.D., Elrick, D.E., 2005. Chapter 6 Measurement and characterization of soil hydraulic properties. In J. Álvarez-Benedí, & R. Muñoz-Carpena (Co-Eds.), *Soil-water-solute process characterization – An integrated approach*. Boca Raton: CRC Press.
- Reynolds, W.D., Elrick, D.E., 2002. 3.4.3.3 Constant Head Well Permeameter (Vadose Zone), in: *Methods of Soil Analysis: Part 4 Physical Methods*, SSSA Book Series. Soil Science Society of America, Madison, WI, pp. 844–858. <https://doi.org/10.2136/sssabookser5.4.c33>
- Reynolds, W.D., Elrick, D.E., 1990. Ponded Infiltration From a Single Ring: I. Analysis of Steady Flow. *Soil Science Society of America Journal* 54, 1233. <https://doi.org/10.2136/sssaj1990.03615995005400050006x>
- Ross, P.J., Haverkamp, R., Parlange, J.-Y., 1996. Calculating parameters for infiltration equations from soil hydraulic functions. *Transport in porous media* 24, 315–339.
- Roulier, S., Angulo-Jaramillo, R., Bresson, L.-M., Auzet, A.-V., Gaudet, J.-P., Bariac, T., 2002. Water transfer and mobile water content measurement in a cultivated crusted soil. *Soil Science* 167, 201.
- Smettem, K.R.J., Parlange, J.Y., Ross, P.J., Haverkamp, R., 1994. Three-dimensional analysis of infiltration from the disc infiltrometer: 1. A capillary-based theory. *Water Resour. Res.* 30, 2925–2929. <https://doi.org/10.1029/94WR01787>
- Smiles, D., Knight, J., 1976. A note on the use of the Philip infiltration equation. *Soil Res.* 14, 103–108.
- Smith, R.E., Smettem, K.R., Broadbridge, P., 2002. Infiltration theory for hydrologic applications. *American Geophysical Union*.
- Stewart, R.D., Abou Najm, M.R., 2018a. A Comprehensive Model for Single Ring Infiltration I: Initial Water Content and Soil Hydraulic Properties. *Soil Science Society of America Journal* 82, 548–557. <https://doi.org/10.2136/sssaj2017.09.0313>
- Stewart, R.D., Abou Najm, M.R., 2018b. A Comprehensive Model for Single Ring Infiltration II: Estimating Field-Saturated Hydraulic Conductivity. *Soil Science Society of America Journal* 82, 558–567. <https://doi.org/10.2136/sssaj2017.09.0314>
- van Genuchten, M.T., 1980. A closed-form equation for predicting the hydraulic conductivity of unsaturated soils. *Soil science society of America journal* 44, 892–898.
- Vandervaere, J.-P., Vauclin, M., Elrick, D.E., 2000. Transient flow from tension infiltrometers I. The two-parameter equation. *Soil Science Society of America Journal* 64, 1263–1272.
- Warrick, A.W., Broadbridge, P., 1992. Sorptivity and macroscopic capillary length relationships. *Water Resources Research* 28, 427–431. <https://doi.org/10.1029/91WR02599>
- Watson, K.W., Luxmoore, R.J., 1986. Estimating macroporosity in a forest watershed by use of a tension infiltrometer. *Soil Science Society of America Journal* 50, 578–582.
- White, I., Sully, M.J., 1992. On the variability and use of the hydraulic conductivity alpha parameter in stochastic treatments of unsaturated flow. *Water Resour. Res.* 28, 209–213. <https://doi.org/10.1029/91WR02198>
- White, I., Sully, M.J., 1987. Macroscopic and microscopic capillary length and time scales from field infiltration. *Water Resour. Res.* 23, 1514–1522. <https://doi.org/10.1029/WR023i008p01514>
- Wu, L., Pan, L., Mitchell, J., Sanden, B., 1999. Measuring Saturated Hydraulic Conductivity using a Generalized Solution for Single-Ring Infiltrometers. *Soil Science Society of America Journal* 63, 788. <https://doi.org/10.2136/sssaj1999.634788x>
- Xu, X., Lewis, C., Liu, W., Albertson, J.D., Kiely, G., 2012. Analysis of single-ring infiltrometer data for soil hydraulic properties estimation: Comparison of BEST and Wu methods. *Agricultural Water Management* 107, 34–41. <https://doi.org/10.1016/j.agwat.2012.01.004>